ROLE OF HUMAN APRATAXIN PROTEIN IN p53-RELATED CELLULAR PROCESSES IN BREAST CELLS

A Thesis Submitted to
the Graduate School of Engineering and Sciences of
İzmir Institute of Technology
in Partial Fulfillment of the Requirements for the Degree of

MASTER OF SCIENCE

in Molecular Biology and Genetics

by
Hülya Doğan

December 2021
İZMİR

ACKNOWLEDGEMENTS

The guidance and patience of my supervisor Assoc. Prof. Dr. Özden YALÇIN-ÖZUYSAL has been invaluable. I would like to offer my special thanks to her for the support and suggestions during the development of this research work.

Also, I would like to thank to my thesis committee members Assoc. Prof. Dr. Gülistan MEŞE-ÖZÇİVİCİ, Prof. Dr. Ahmet KOÇ and Assoc. Prof. Dr. Özden YALÇIN-ÖZUYSAL.

I would like to thank to Prof. Dr. Engin ÖZÇİVİCİ and Assoc. Prof. Dr. Gülistan MEŞE-ÖZÇİVİCİ for their contribution to this project.

Furthermore, I wish to thank to Prof. Dr. Bünyamin AKGÜL, Prof. Dr. Devrim PESEN-OKVUR, Prof. Dr. Hüseyin Çağlar KARAKAYA and IYTE, Biotechnology and Bioengineering Research and Application Center for their laboratory resources and facilty support.

It is a great pleasure and relief that I complete this thesis. I could not have achieve this without the support of my laboratory colleagues Eda EFE, Zehra Elif GÜNYÜZ, Yağmur Ceren ÜNAL, Aslı KISIM, Kübra TELLİ, Perge Bilgesu TOSUNOĞLU and Burcu Fıratlıgil-YILDIRIR. They kept me going even in difficult moments. I feel so blessed to have friends who walk beside you and are ready to hold you when you fall. No words can express my gratitude. Moreover, the support and kindness of Mustafa İLHAN has been very much appreciated.

My sincerest thanks to Büşra KORKMAZ, Türkan DEMİRCİ, Tuğçe KORKMAZ, Orhan Kerim İNCİ, Gözde DERELİ and Gözde KIRIM for being such amazing and motivating friends. Thank you for making the ordinary moments in life extraordinary.

I express my deepest gratitude to my parents and grandparents for their encouragement and constant love. This journey would not have been possible without the support of my family.

Funding for this project was received from TÜBİTAK (Project Number:117Z990).

ABSTRACT

ROLE OF HUMAN APRATAXIN PROTEIN IN p53-RELATED CELLULAR PROCESSES IN BREAST CELLS

Aprataxin encoded by APTX, which is the human homolog of yeast HNT3, reverses adenylation damages emerged from abortive DNA ligation during ribonucleotide and base excision repair. Thus, it corrects AMP-modified nucleic acid termini and protects genome integrity as a DNA ligase "proofreader". Role of HNT3, which is a candidate p53-related gene, against DNA oxidative and alkylating damage indicates its antioxidant importance. Besides, previous studies demonstrated that absence of Aprataxin gives rise to ROS generation and oxidative stress in addition to mitochondrial dysfunction. Also, role of Aprataxin in drug and radiotherapy sensitivity was shown in many cancer.

Since conformation of cysteine residues in p53 DNA-binding domain can be modified by oxidizing environment, functionality can be influenced by defective APTX. Although p53-Aprataxin interaction has been shown by co-immunoprecipitation, effects of APTX on p53 pathway were not studied.

Aim of this study is to investigate Aprataxin-driven changes in p53-regulated processes in p53 wild-type cells through. According to results, Aprataxin overexpression leads to cell cycle arrest in low stress levels. However, it triggers cell death against induced stress in MCF10A cells. Moreover, apoptotic assay on MCF10A APTX Crispr cells indicated elevated level of basal cell death. Also, expression analysis of p53 targets in APTX knockdown MCF7 cells revealed that extrinsic apoptosis pathway might be induced.

Consequently, these results help us to gain insight into how Aprataxin affects activity of p53 pathway. Further investigation providing stress accumulation based assays and protein level analysis is needed to figure out whether resulting changes are p53-dependent or not.

ÖZET

MEME HÜCRELERİNDE p53 TARAFINDAN DÜZENLENEN HÜCRESEL SÜREÇLERDE İNSAN APRATAKSİN PROTEİNİNİN ROLÜ

HNT3 antioksidan geninin insandaki homoloğu APTX geninden üretilen Aprataksin, adenilat içeren abortif DNA ligasyon ara ürünlerine etki ederek verimli bir şekilde yeniden birleşebilen terminaller oluşturur. Böylece DNA hasarını engellerler. Ayrıca birçok DNA tamir proteini ile de etkileşim halindedir. Bunlar arasında hücre döngüsünü, apoptozu ve DNA tamirini kontrol eden p53 de bulunmaktadır. p53 fonksiyonunu, stabilitesini ve katlanmasını belirleyen DNA-bağlanma alanı birçok sistein kalıntıları barındırmaktadır. Bu kalıntılar arası bağlar oxidatif ortamda dönüşerek protein konformasyonunu değiştirir. Bu sebeple antioxidan Aprataksin, p53 üzerinden bağlantılı yolakları regüle edebilir.

Önceki çalışmalar göstermiştir ki Aprataksin yokluğu reaktif oksijen türü seviyesinde artışa neden olurken aynı zamanda mitokondrianın işlevselliğini bozmuştur. Beyin ve kas hücrelerinde yıkıcı etkilere neden olan bu genin mutasyonu meme hüclerinde çalışılmamıştır.

Bu çalışmanın amacı p53'e bağlı hücresel süreçlerin Aprataksin temelli değişimlere karşı oluşturduğu farklılıkları ortaya çıkarmaktır. Aprataksin fazla ekspresyonunun MCF10A hücrelerinde düşük stres koşullarına karşı hücre döngüsünün ilerleyişini durdurduğunu tespit edilmiştir. Fakat aynı hücre hatlarında indüklenmiş stres ortamında apoptozun tetiklendiği görülmüştür. Ayrıca MCF10A APTX Crispr hücreleriyle yapılan apoptotik ölçümlerde kontrole kıyasla yüksek seviyede bazal hücre ölümü gözlemlenmiştir. MCF7 APTX Crispr hücrelerinde ise p53 hedef genlerinin ekspresyon seviyesi analizi apoptozun ekstrinsik yolağında potansiyel bir değişimi işaret etmektedir.

Sonuç olarak, bu araştırmanın bulguları Aprataksin'in p53 yolağını nasıl etkilediğini anlamamıza yardımcı olmaktadır. Hem stress seviyesine hem de protein düzeyindeki farklılıklara odaklanan daha detaylı incelemeler gelecekteki çalışmalara eklenmelidir.

TABLE OF CONTENTS

LIST OF TABLES

Table **Page**

LIST OF FIGURES

Figure **Page**

Figure **Page**

CHAPTER 1

INTRODUCTION

1.1. p53 Transcription Factor

p53 transcription factor encoded by TP53 gene located on chromosome 17 is a key tumor suppressor and name indicates molecular weight. 43.7 kDa is the actual molecular mass based on calculation of aminoacid structure but SDS-PAGE analysis showed 53 kDa due to proline residues causing slower separation.[1] In 1979, a couple of independent research groups identified a protein bound to T-antigen of SV40 strain infected cell lines after co-immunoprecipitation.[2] Since this strain has a role in development of tumors, p53 was accounted as an oncogene. This prediction was supported with the findings point out the high amount of p53 in many cancers. However, further studies revealed mutations of p53 causing single base substitution or deletion in various tumor types. Knock out mice with no p53 expression were also tumor prone therefore it is characterized as a tumor suppressor gene in 1989.[3]

p53 is involved in the regulation of growth arrest, angiogenesis, DNA repair, antioxidant response, metabolic processes and apoptosis. Although p53 expression in normal cells is detected at low levels, stress conditions such as oncogene activation, toxicity, ultraviolet, hypoxia, lack of nutrients and excessive activation of telomerase increase its production. Activation of p53 target genes triggers repair mechanisms and delay in the cell cycle which prevents accumulation of mutations. If this attempt cannot repair the damage, those cells are forced to encounter apoptosis. Considering requirement of p53 to impede development of tumors, it is also called the "guardian of the genome."[4]

Cell cycle checkpoints are one of the defense mechanisms to recognize damages and preserve cellular state. p53-mediated induction of p21 can prevent transition

between cell cyle stages. p21 brings about G1/S or G2/M arrest through targeting cyclin dependent kinases, CDK2 and CDC2 respectively. 14-3-3 and GADD45 proteins which are transcriptional targets of p53, might interrupt the progression in G2/M checkpoint by CDC2 sequestration.[5] On the other hand, 14-3-3 acts as a tumor growth-suppressor responding to cancer metabolic reprogramming and migration.[6] Pro-apoptotic proteins BAD, PUMA and KILLER which are also p53-downstream targets, stimulate intrinsic apoptosis pathway to handle cellular stress.[7]

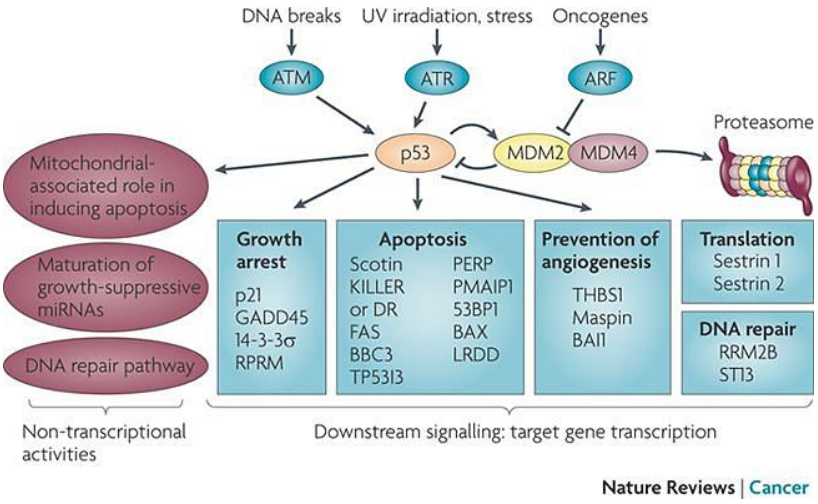

Figure 1.1 p53 downstream targets generate a network of biological interactions which transforms stress factors into responses using DNA repair, cell cycle arrest or apoptosis. [8]

p53 can orchestrate repair processes such as base excision repair (BER) in coordination with APE1/Ref1 endonuclease and DNA polymerase β. For instance, it enforces BER during G_0-G_1 phases but loses this effect and inversely cells undergo apoptosis along G_2-M stages of cell cycle.[9] Aside from this direct DNA binding for recovery of particular DNA lesions, greater part of p53 downstream targets participate in repair machineries.[10] However, tissue of origin and microenvironment modulate response of multifunctional p53.[11] Modification patterns inflicted by stress factors might also determine cell fate.[12]

1.1.1. Modes of p53 Regulation

Majority of factors affecting activation of p53 protein is on the basis of post-translational regulation resulted from stress exposure. Although RNA binding proteins and untranslated regions play role in mRNA stability, modifications determine functionality in protein level and its interacting partners. While phosphorylated regions around N-terminus are crucial for binding to its negative regulator Mdm2, certain hot-spots for phosphorylation and acetylation along C-terminus enables DNA binding. Mdm2 orchestrates proteosome-mediated degradation through ubiquitylation.[13] Phosphorylated residues accompanied by activation of distinct kinases stabilize p53 because Mdm2 binding is hindered. Active p53 occupies its binding site in tetrameric form.[14] Moreover, redox-based control mechanisms contribute the stabilization of p53 protein.[15]

1.1.2. Redox regulation of p53

Cysteine residues connected by zinc ion within DNA-binding domain are critical for a proper p53 folding. This zinc atom keeps p53 at reduced state but oxidizing environment targets zinc-coordination center inducing disulfide bonds. Therefore, reducing cellular environment is essential to maintain the bridge between DNA and p53.[15] Also, redox-dependent protein APE1/Ref-1 tunes up p53 activation. This pair reduces reactive oxygen species (ROS) and regulate metabolism to maintain homeostasis. APE1/Ref1 engaged with p53 triggers expression of p21, a CDK inhibitor and accordingly cell cycle arrest in severe conditions. However, it serves as co-repressor for p21 proximal promoter region in case of p53-null cells which explains enhanced proliferation in p53 inactivated tumor cells with APE1/Ref1 overexpression.[16] Additionally, another redox-active protein Thioredoxin both being associated with APE1/Ref1 or not, promotes p53 DNA binding capacity.[15] Those findings suggest that p53 tends to be regulated by redox active proteins.

Table 1.1: Relative p53 activities of mutants acquired from p53 reporter system in yeast [17]

ORF	**Gene**	**Human Homolog**	**p53 activity (%)**
WT	-		100
YKL212W	SAC1	SACM1L	50,6
YOR258W	HNT3	APTX	26,2
YLR244C	MAP1	METAP1	16,5

A recent study carried out on *Saccharomyces cerevisiae* as a model organism focused on screening thiol-dependent antioxidant gene mutants that might affect p53 activity. A LacZ reporter system which can be inducible by p53 was used to determine yeast mutants that decrease p53 activity. Exogeneously introduced human p53 gene followed by beta-galactosidase encoding gene was integrated into yeast strains.[17] Consequently, in *Saccharomyces cerevisiae* three candidate genes were identified as regulators of p53 activity. Regulation of p53 by the candidate genes in human needed further investigation.

1.2. Aprataxin: Domains and Interacting Proteins

Aprataxin encoded by *APTX* gene is a Histidine Triad (HIT) superfamily protein with deadenylase function. In addition to nucleus and nucleolus, its presence in mitochondria has been shown.[18] Although 13 isoforms resulting from alternative splicing have been identified, 2 isoforms named as long (39kDa) and short (20kDa) form are dominantly detected in the cells. All consists of a central HIT domain controlling nucleotide hydrolysis and a C-terminal zinc finger (ZF) domain provides recognizing

the target region and binding to DNA. Various mutations in HIT and/or ZF domains of Aprataxin leads to a neurodegenerative disease, Ataxia-ocular motor apraxia 1 (AOA1) and this consequence points out their significance in catalytic activity. People suffer from this disorder exhibits involuntary eye movement, poor muscle coordination and problems in speech. Besides, additional AOA1 symptoms are disruption of neurons in cerebellum, low albumin levels and high cholesterol. Other AOA types are linked to abnormalities in different genes.[19]

Nuclear long form of this DNA repair protein interacts with XRCC1 and XRCC4 (ligase cofactors), which are key proteins participate in single strand break (SSB) and double strand break (DSB) repair complexes respectively, through N-terminal forkhead-associated (FHA) domain. The cytoplasmic short form lacking of FHA domain does not interact with XRCC1 or XRCC4.[20] This domain is also required for interaction between APTX and Mediator of DNA-damage checkpoint protein 1 (MDC1) which is also a distinct DSB repair protein.[21] Further, p53 and PARP-1 binds to APTX associating with FHA and HIT domains.[22] Codependency of repair proteins for their expression has been observed in this network. Diminished levels of APE1 and PARP-1 were detected in uncorrected AOA1 cells whereas their expression returned to normal levels in rescued cells. This study highlighted that Aprataxin adjusts expression levels of the proteins contribute to DSB repair and apoptosis. At the same time, PARP-1 controls the amount of Aprataxin.[23]

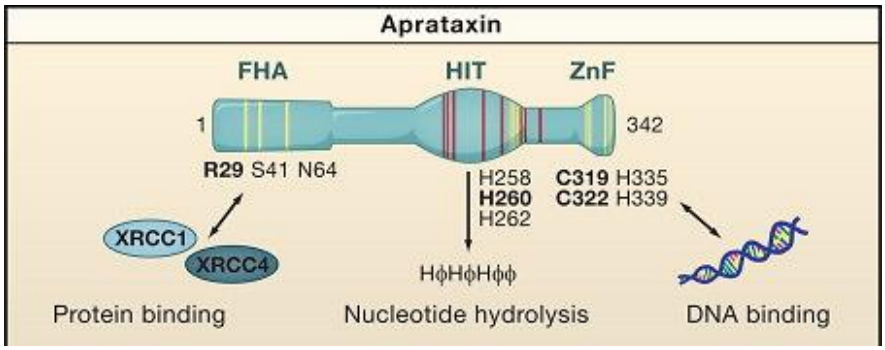

Figure 1.2 Domains of Aprataxin protein and their corresponding functions. [24]

Cytoplasmic isoforms of Aprataxin are mainly present in neuron-like cells and they cannot collaborate with DNA repair proteins due to absence of FHA domain. Mitochondria targeting sequence is abundant in brain transcriptome so Aprataxin isoforms are usually located inside the mitochondria in the brain. Although they are involved in maintaining mtDNA integrity, they do not take part in repair.[18]

It has been previously suggested that Aprataxin is primarily localized in nucleolus where ribosome generation is managed. rDNA damage would disorganize cell growth and proliferation, stalling the transcriptional machinery. As expectedly, nucleolin, nucleophosmin and upstream binding factor 1 (UBF-1) which are engaged with rRNA transcription and maturation are among its interacting partners. However, no failure was addressed along rRNA biogenesis in AOA1 cells. When transcription was blocked by actinomycin D, Aprataxin and UBF-1 were distributed into peri-nucleolar caps confirming genomic stress. Thus, aprataxin may protect rDNA against certain breaks instead of regulating rRNA metabolism.[25]

1.2.1 Functions of Aprataxin

The catalytic feature of Aprataxin is adjusting the abortive ligation intermediates at the end of replication or repair. ATP dependent ligases transfer AMP to 5' phosphate end so 5'AMP becomes available for 3'OH to attack to accomplish the ligation. If this last attacking step is interrupted due to damages, AMP must be removed to keep a proper architecture for an effective nick-sealing step. Aprataxin is not strictly necessary for a regular ligation process while replacing AMP from DNA ligase III but it facilitates efficiency of the rejoining. However, sensitivity of DNA ligase against damages during BER, Ribonucleotide excision repair (RER) and DSB repair generates the need of Aprataxin for another round of reaction to seal the nick. HIT loop (his260) and helical wedge of Aprataxin mediates hydrolysis of the bulky adenylated nucleotide groups and favors nicks DSB nicks as substrate compared to ssDNA.[24] Existing research has established that Aprataxin takes role in elimination of those aberrant adenylated

intermediates emerged from oxidizing, alkylating environment to protect genome integrity.[26]

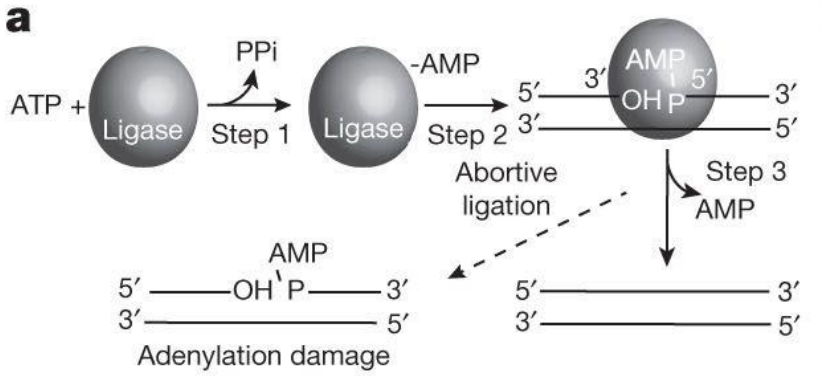

Figure 1.3 Adenylation damage stems from abortive ligation with ATP-dependent ligase. [27]

The loss of Aprataxin might be compensated by long patch BER (LP-BER) and homologous recombination in proliferating cells. Since those processes are not so effective in non-replicating cells, pol β-dependent LP-BER operates restoring deadenylated substrate for ligase. This complementation may clarify insensitivity against DNA damaging agents and absence of cancer susceptibility and immunodeficiencies in AOA1 patients. However**,** DNA polymerase gamma functions as dominating polymerase in mitochondria, does not have this property. Therefore, abnormal intermediates in mitochondrial genome are not resolved by an back-up mechanism.[28] Mitochondria quality is crucial in neuronal and muscle cells with intense ATP consumption. Especially, dynamic oxygen metabolism in brain makes neurons exposed to radical attack. This renders accumulation of overadenylated termini detrimental for neuron and muscle cells with mutant Aprataxin.[29]

1.2.2. Aprataxin and Oxidative Stress

Eventhough some studies proposed sensitivity against genotoxic agents or delayed repair mechanism in APTX defective cells, response and repair processes are appeared to be unaffected according to other studies. Lower tolerance of AOA1 fibroblasts with p.W279 mutation to DNA damaging agents H_2O_2, MMS (methyl methanesulfonate) and etoposide was reported.[30] A notable example of increasing H_2O_2 and MMS sensitivity was also indicated in APTX depleted HeLa cells through disorganization of XRCC1 stability.[22, 31] These observations match the results indicating the interplay between Aprataxin and SSB proteins. Although XRCC4-Aprataxin interaction involved in DSB repair was found, there is no evidence for defective DSB repair or an overt phenotype developed by APTX loss in cells or mice.[21, 32, 33] These contrary results might be originated from cell type or position and type of the mutations. Altered protein stability with specific mutations may lead to this variation.

Moreover, the effect of APTX disruption is related to how common damage occurs in the cellular level. Accumulation of lesions emerged from increasing passage number uncovered the impact of APTX deletion when cells exhibited enhanced senescence in a stress environment with low O2 supply. Thus, importance of the stress exposure in APTX inactivated cells was confirmed.[34]

Considering mitochondria-based abnormalities in Aprataxin-deficient non-neuronal cells, transcriptional regulation affected by APTX loss was presumed. Understanding the mitochondrial dysfunction resulted from differences in APE1/NRF1/NRF2 pathway implicated the crosstalk between nucleus and mitochondria. The study demonstrated that absence of Aprataxin gives rise to reduction of this pathway associated with CoQ10 biosynthesis. Since CoQ10 works as an antioxidant and an electron carrier playing role in oxidative phosphorylation, it supports the outcomes of Aprataxin deficiency including impaired mitochondrial function and mitophagy followed by robust ROS generation and elevated levels of oxidative DNA damage in HeLa cells and AOA1 fibroblasts.[35]

In general, fusion proteins are upregulated in cancer to lessen accumulated defective mitochondrial particles and contribute to avoid apoptosis. Aberrant

mitochondrial morphology and inefficient mitophagy are linked to decreased OPA1 fusion protein in APTX knockout U2OS human bone osteosarcoma cells and HEK cells in addition to AOA1 patient cells. Dysregulation of respiration capacity, ROS overproduction, changes in mitochondria morphology and damaged mitophagy correlate with expected results regarding the role of OPA1 in inner mitochondrial membrane formation. [29]

1.3. Interaction between p53 and Aprataxin

Destabilization of repair proteins is likely to be interdependent on account of their multiprotein complex formation. Conformational change of proteins in contact can differ the nature of the other associated proteins. For instance, correlation between absence of Aprataxin and enhanced nucleolin degradation reflects that Aprataxin may coordinate nucleolin stability. Improved steady-state levels of nucleolin arised from Aprataxin overexpression approved this impact. A similar interplay might occur with other related complexes.[25]

Aprataxin-p53 interaction has been shown by co-immunoprecipitation and extensive SSB stems from H_2O_2 treatment strengthens their binding via p53 stabilization.[22] However, detailed research with structural biology approaches needs to be done to understand their interaction. Furthermore, oxidizing environment is capable of modifying p53 DNA-binding domain through determination of cysteine residue conformation as explained in section “Redox regulation of p53”. Since several reports identified p53-protein interactions through specific DNA binding core domain, p53 functionality can be altered by defective APTX. [11, 36, 37]

1.4. Aprataxin and Cancer

Resistance against drugs and/or radiotherapy is a critical bottleneck in cancer therapy so researchers study to overcome this global health concern. Determination of

biomarkers provides advantages for precision medicine. Previous studies showed that Aprataxin participates in those resistance mechanims in various cancer types. Microarray and histological analysis of colorectal cancer samples suggested that patients with low Aprataxin level are more likely to respond to camptothecin and its derivatives. It is worth noting that clinical evaluations validated that low APTX expression in tumor significantly improved survival rates.[38] Besides, radioresistant cervical cancer cells were sensitized by activation of miR-424 expression targeting Aprataxin. Ectopic miR-424 expression paves the way for irradiation-induced apoptosis and G2/M arrest. [39]

Thereby, p53-Aprataxin linkage might be promising to enlighten the resistance characteristics of cancer cells and understand how to get cancer cells weakened targeting APTX. If the role of this interaction on cell cycle and/or apoptosis can be figured out, we can address ways to rescue the tumor-suppressing function of p53.

1.5 Aim of the study

Despite existing research implied the interaction between Aprataxin and p53, there is no experimental data illustrating APTX-driven changes on p53 activity. Therefore, the goal of this study is to investigate whether APTX affects p53-regulated processes. In order to reach this goal, APTX was overexpressed or disrupted in breast cell lines carrying wild type p53 and then p53-related processes such as cell cycle, proliferation and apoptosis were analyzed.

CHAPTER 2

MATERIALS AND METHODS

2.1 Cell culture

Non-tumorigenic human mammary epithelial cell line MCF10A (American Type Culture Collection, ATCC) were grown in high glucose DMEM/F-12 (Thermo-Fisher Scientific, Cat No: 31330038) supplemented with final concentrations of 5% Donor Horse Serum (Gibco, Cat No: 16050-122), 20 ng/ml EGF (Sigma, Cat No: E9644-5MG), 0.5µg/ml Hydrocortisone (Sigma, Cat No: H0888-1G), 10µg/ml Insulin (Sigma, Cat No: I1882-100MG), 100 ng/ml Choleratoxin and 1% Penicillin/Streptomycin mixture (Thermo-Fisher Scientific, Cat No: 15140-122). Mammary adenocarcinoma cells MCF7 (ATCC) and human embryonic kidney (HEK) cells 293T (ATCC) were cultured in high glucose DMEM (Sigma, Cat No: D6429) with addition of 10% Fetal Bovine Serum (Thermo-Fisher Scientific, Cat No: 10270106) and 1% Penicillin/Streptomycin mixture (Thermo-Fisher Scientific, Cat No: 15140-122). All cell types were cultivated in a humidified incubator set to 37°C and 5% CO_2 conditions.

2.2 Plasmid Construction

To generate APTX overexpressing cells, V5 tagged pLX304-APTX plasmid was used while V5 tagged pLX304-LacZ plasmid was used for the control cell line. APTX knockdown was achieved performing Crispr/Cas9 one-vector approach. 4 gRNA pairs targeting APTX gene were obtained via online tools, CHOPCHOP and Broad Institute's sgRNA designer minimizing off-target possibility. Overhangs were designed to be

complementary for BsmBI cut ends. Annealed sgRNA pairs were inserted into BsmBI-digested lentiCrispr V2 vector which contains U6 promoter to maintain an efficient expression and integrated Cas9 sequence. Positive clones with expected PCR products size (200-300kb) were selected. Crispr plasmid construct was validated by Sanger sequencing of the region using hU6-F primer. Non-targeting sgRNA plasmid called NTL was used to create control cell lines for Crispr cells.

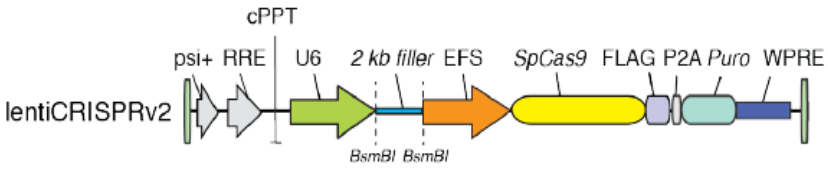

Figure 2.1 Map of lentiCrisprV2 plasmid designed by Zhang lab [40]

2.3 Virus Production

$3x10^6$ cells of HEK-293T cells were cultured on 10 cm plate for generation of viruses. When the cells had the 80-90% confluency over the plate, transfection was carried out using several plasmids and Fugene HD (Promega, Cat No: E2311). 1.3 µg of packaging vector psPAX2 0.7 µg of envelope vector pMD2.G and 2 µg of related plasmid were mixed in DMEM serum-free medium. Tranfection reagent was added as 3 µl for 1µg of plasmid. After 30 minutes incubation at room temperature, this serum-free medium was put onto cell medium in droplets. Medium was exchanged with complete medium at 24 hours post-transfection. Viral supernatant was collected after 48 and 72 hours of transfection. Virus aliquots were stored at -80°C.

2.4 Lentiviral Tranduction

To get stable cell lines with overexpressed APTX and CRISPR/Cas9 mediated disrupted APTX expression, lentiviral transduction protocol was used. $250x10^3$ cells of MCF10A cell line and $300x10^3$ cells of MCF7 cell line were cultured on 6-well plate 24 hours prior to infection. lacZ (control), plx304-APTX or CrisprV2-APTX sgRNA viruses mixed with polybrene (final 8µg/ml) were used for corresponding infection of cells. Then, cells were centrifuged at 2500 rpm for 2 hours at 32°C for a higher transduction efficiency. Next day, medium was changed with complete growth medium. After 3 days of transduction, selection with blasticidin (4 µg/ml) or puromycin (2 µg/ml) containing medium was started for overexpression and knockdown cells respectively.

2.5 RNA Isolation and cDNA synthesis

Total mRNA of the cells were isolated according to kit recommendations (NEB, Cat No: T2010S). After concentration of obtained RNA was measured, complementary DNA was synthesized in reaction containing 1µg RNA, random primers, reverse transcriptase, RNAse inhibitors and dNTP. (Thermo Scientific, Cat No: K1622)

2.6 Quantitative Real Time RT-PCR (RT-qPCR)

Gene expression levels were determined by SYBR green based RT-qPCR. cDNA which is the template and specifically designed primer pairs are added into SYBR green mix (RealQ, Cat No: APQ-A323402**)** including Taq polymerase, dNTP, buffer, SYBR green dye. The used primer sequences are shown in Table 2.1. Cycle threshold (Ct) values of triplicate samples representing amplification levels were measured on

Roche, Light Cycler 96 Real time PCR detection system and their mean was calculated. After normalization was applied by substracting Ct values of TATA box binding protein (TBP) in each sample, delta -delta Ct method was used to uncover the fold changes. For statistical analysis, two-tailed student t-test was selected.

Table 2.1: 5’ Primer sequences used in RT-qPCR are listed. F: Forward, R: Reverse

Target gene	**5’ Sequence**
PUMA-F	GACGACCTCAACGCACAGTA
PUMA-R	CTGGGTAAGGGCAGGAGTC
BAD-F	CGGAGGATGAGTGACGAGT
BAD-R	CCACCAGGACTGGAAGACTC
KILLER-F	GATGGTCAAGGTCGGTGATT
KILLER-R	CCCCACTGTGCTTTGTACCT
14-3-3-F	ACCCAATTCGTCTTGGTCTG
14-3-3-R	GCTTCATCAAATGCCGTTTT
GADD45-F	GGAGGAAGTGCTCAGCAAAG
GADD45-R	ATCTCTGTCGTCGTCCTCGT
p53-F	AAGACCCAGGTCCAGATGAAGC
p53-R	GAAGGGACAGAAGATGACAGGG
p21-F	
p21-R	
APTX-F	TGCAGGTTTACAAAGATGAGCAGG
APTX-R	GCCACAGCCTTCAGACTGGAAATG
U-6 F	GAGGGCCTATTTCCCATGATT

2.7 Protein Isolation and Quantification

Lysis mixture containing RIPA buffer, 1X Protease inhibitor, 1mM DTT, 1mM $NaVO_4$ and 50mM NaF was added onto thawn cells on 6-well plate. Adherent cells were collected into eppendorf tubes after detachment by scraper. Transfered cells were passed through syringe and incubated on ice for 20 minutes. Samples were placed into precooled rotor and centrifuged at 14000 rpm at 4°C for 20 minutes. Total protein remained in the supernatant was taken into a new eppendorf tube. For quantification of protein amount, Bradford assay was performed. BSA standards at 0.5, 1, 2, 4 and 8 mg/ml concentration were prepared. Each standard was mixed with 800µl distilled water and 200µl of 5X Bradford. Spectrophotometric analysis at 595nm was taken place in 1cm cuvettes. The machine calculated the concentration of samples based on the equation resulted from the calibration curve.

2.8 Western Blot

When SDS-PAGE was solidified totally, proteins mixed with loading dye denatured at 95°C for 5 minutes were loaded in equal amount (30-60µg). Resolved proteins on gel were moved onto PVDF membrane by wet transfer. In this method, Gel/Membrane/Filter Paper sandwich is put into tank full of transfer buffer across a vertical electic field at 40V for 3hours. Blocking step was accomplished by incubation in 5% milk powder in 1X TBS-T overnight at 4°C. Then, membranes were treated with 1:1500 APTX primary antibody (ThemoFisher, Cat No: PA5-41687) or 1:1000 V5 primary antibody (Thermo-Fischer Scientific, Cat No: PA1-993) in 5% milk powder in 1X TBS-T overnight at 4^0C. Next day, 10 minutes washing step via 1X TBS-T was performed for 3 times and membranes were incubated with 1:2000 secondary antibody (CST, Cat No: 7074S) in 1X TBS-T for 2 hours at room temperature. After washing procedure was repeated, protein of interest was detected using Chemiluminescence ECL

substrate (Bio-Rad, Cat No: 1705061) by Image analyzer. Intensity levels plotted by ImageJ were used to analyse the image quantitively**.** Signal of β-actin housekeeping protein was used to check equal loading and normalize intensity differences. LacZ producing cell line transduced with backbone vector was the control to achieve an accurate comparison. Two tailed Student's t-test was used to calculate statistical significance.

2.9 MTT Assay

This assay was carried out to report cell viability changes since metabolically active cells are able to convert yellow 3-(4,5-dimethythiazol-2-yl)-2,5-diphenyl tetrazolium bromide (MTT) into purple formazan. Seeding of $9x10^3$ MCF10A cells or $5x10^3$ MCF7 cells onto each well of 48-well plate was followed by MTT assay at day 1, 3, 5 and 7. After incubation at 37°C for 4 hours with 10% MTT in complete medium was done, solution was aspirated and cells formazan crystals were soluabilized within 100µl DMSO were transferred into 96-well plate for OD measurement. Spectrometric data from Thermo Multiskan Spectrum was blanked against DMSO. Also, 650nm noise was substrated from 570nm.

2.10 Trypan Blue Staining/ Cell Counting

$9x10^3$ MCF10A cells and $5x10^3$ MCF7 cells were seeded on 48-well plate as 3 replicate for each condition. Cells were trypsinized and counted on hemacytometer at day 1, 3, 5 and 7. Each replicated was counted 2 times. Trend in growing period was plotted based on average of those data.

2.11 Annexin V Assay

250k MCF10A cells and 300k MCF7 cells were seeded onto 6-well plates. After 48h incubation at 37°C, 2.5 µM Doxorubicin (CST, Cat No: 5927S) or 20µM of Cisplatin (Toronto, Cat No: C499500) was added into culture medium. For control, cells were treated with same volume of DMSO or 0.9% NaCl which is the solvent for the drug. 16 hours treatment was followed by trypsinization. Harvested cells were washed via PBS and centrifuged at 800 rpm for 5 minutes. Pellet was resuspended in 1ml of 1X Binding Buffer (ABP, Cat No: A026). Cells were counted and 10^6 cells/ml was prepared. 50µl was transfered to new eppendorf tubes for each condition. Cells were incubated with 2.5 µl FITC and 1µl PI (ABP, Cat No: A026) at room temperature for 15 minutes in the dark. Finally, sample was mixed with 200µl 1X Binding Buffer. Apoptotic cells were detected through flow cytometry, BD software.

2.11 Propidium Iodide Staining

$80x10^3$ MCF10A cells and $150x10^3$ MCF7 cells were plated on 6-well plates. At day 3, harvested cells were centrifuged at 1200 rpm during 10 minutes. Pellets in falcon preserved on ice were resuspended with 1ml of cold PBS after aspiration. 4 ml of cold 100% ethanol was subsequently added and mixed. Resulting suspension was stored at -20°C minimum overnight and up to 1 year/month. At experiment day, centrifugation at 1500 rpm for 10 minutes and 2000 rpm for 1 minute was performed at 4C successively. Supernatants were discarded and each precipitate disolved in 1 ml of cold PBS was transferred into separate eppendorf tubes. Washing step was completed via spinning at 1500 rpm for 10 minutes at 4°C and supernatants were drawn by pipette. Finally, cells were treated with 200µl of 0.1% Triton X-100 in PBS and 20 µl of RNase A (final 200µg/ml). When incubation at 37°C for 30 minutes had ended, 20µl of PI (1mg/ml) was mixed with solution. Required conditions including room temperature and dark were maintained for at least 15 minutes before measurement BD original software with

BD FACS Canto flow cytometry. Two-tailed student t-test method was used for statistical analysis.

2.12 Bromodeoxyuridine (BrdU) Staining

$350x10^3$ cells/well was seeded on 6-well plates where cover glasses positioned. When cells are confluent, 20μM BrdU was added to media. After 2 hours, medium was aspirated and cells were washed twice by adding PBS. 4% PFA was utilized for fixation step. For permeabilization, cells were subjected to 1.5M HCl for 30 minutes. To block non-specific binding, treatment with 5% NHS in 0.2% Triton X-100 was performed. Next, cells were incubated with BrdU antibody (CST, Cat No:5292S) prepared as 1:1000 in 2%NHS in 1% Triton X-100 overnight. When 3 repeats of PBS wash was completed, mix containing 1:1000 DAPI stain and 1:600 secondary antibody (CST, Cat No: 7074S) in 2% NHS in 1% Triton X-100 was used for 2 hours incubation. Following to wash steps, cells were mounted on a microscope slide. Fluorescent images were recorded using an Olympus fluorescent microscope. For each trial, negative controls were conducted to indicate the absence of nonspecific binding of primary antibody. At least three different regions were measured in each sample. Statistical test was performed by using a two-tailed Student's test.

CHAPTER 3

RESULTS

3.1 APTX overexpression in MCF10A was confirmed both in mRNA and protein level

APTX cDNA ORF was integrated by lentiviral-based delivery to ensure excessive expression of APTX. Positive clones with transgene integration were enriched with antibiotic selection to get stable cell population. While significant overexpression in transcriptional level was verified through RT-PCR (Figure 3.1), density of V5-APTX protein specified by APTX antibody exhibited 3.5 times more elevated APTX expression in protein level of MCF10A cells. Aprataxin band identified by V5 antibody also supported this upregulation (Figure 3.2A and B).

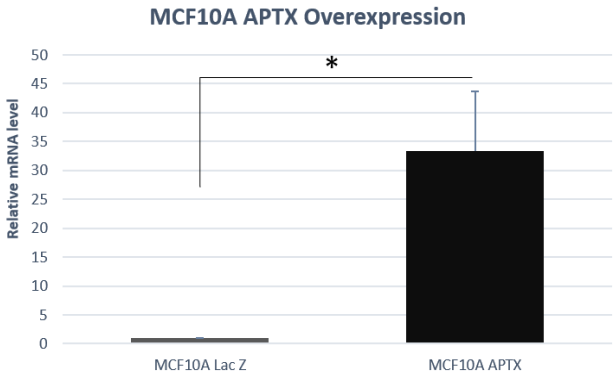

Figure 3.1 Expression analysis of stable MCF10A Aprataxin overexpression cells via quantitative RT-PCR confirmed the lentiviral transduction. TBP expression was measured for normalization. (n=3) (* $p<0.05$)

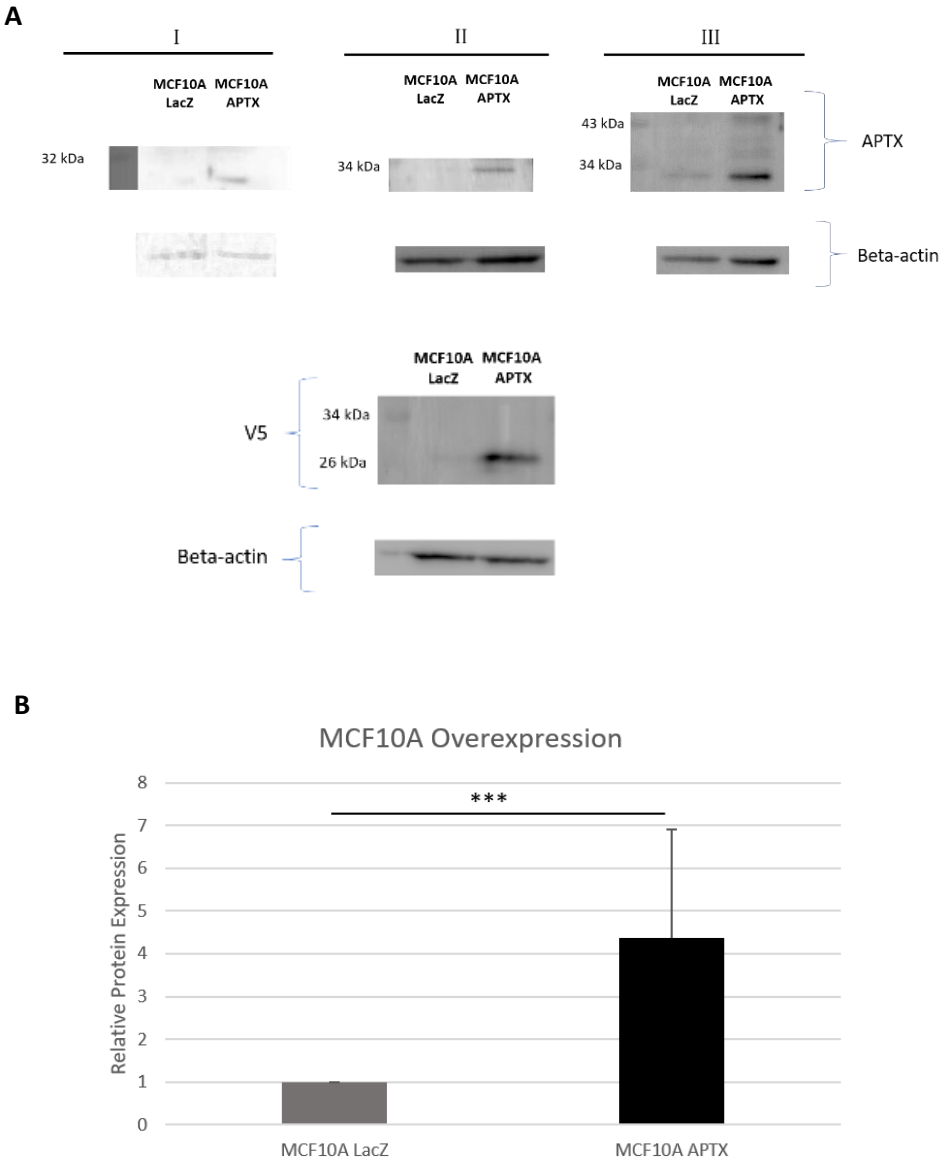

Figure 3.2 Increased Aprataxin protein levels in stable MCF10A APTX overexpression cell lines. A. Western blot results detected with APTX antibody proved the elevated amount of 30 kDa Aprataxin isoform in three independent experiments. V5 antibody also demonstrated the APTX overexpression in representative image at bottom. B. Quantification was achieved by comparing APTX antibody intensities which normalized with β actin levels. (n=3) (***p<0.005)

Observed band for V5 tagged protein was around 30 kDa and this is a rather unexpected result since abundant isoform of Aprataxin is 40 kDa. Although protein

molecular weight calculator based on cDNA sequence estimated 37.69 kDa, Aprataxin can be truncated with cell-specific modification.

3.2 APTX overexpression promotes cell growth

p53 acts as a regulator of growth and proliferation capacity of cells. Hence, promising interaction between p53 and Aprataxin can potentiate role of APTX in cellular growth. Therefore, the impact of APTX upregulation on viability and proliferation rate was examined. MTT assay and Trypan counting were carried out in MCF10A cells. Relative growth was plotted showing signal obtained in each day. Significantly higher viability was found at day 3 and 7 based on MTT results. (Figure 3.3) Trypan counting also approved this finding with significantly higher number of cells at day 7 for APTX overexpressing cells. (Figure 3.4)

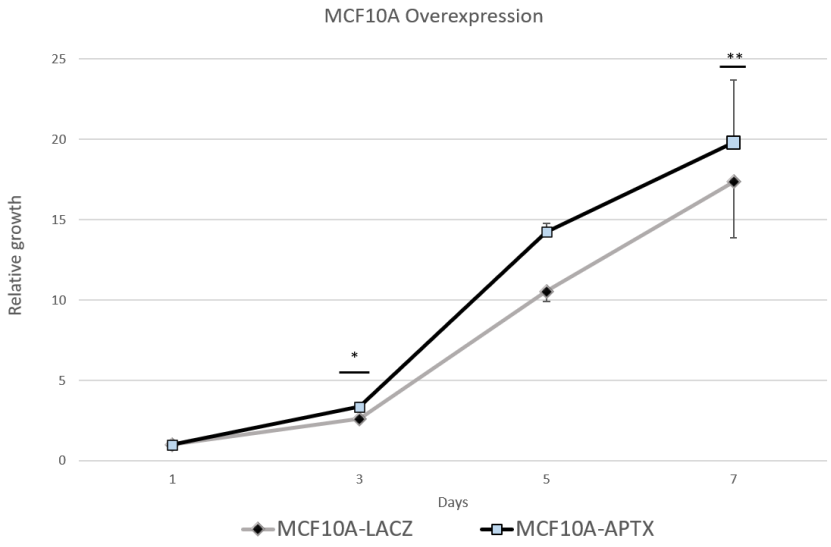

Figure 3.3 Cell viability of MCF10A APTX overexpression cells was investigated at different time points performing MTT assay. Absorbance of each day was normalized to Day 1 of corresponding cell line. (n=2) (*p<0.05, **p<0.01)

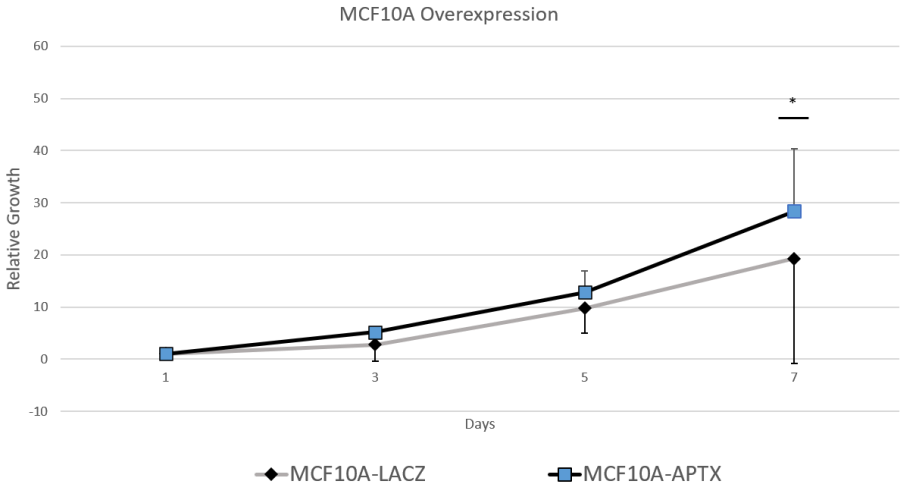

Figure 3.4 Cell viability of MCF10A cells through Trypan counting. Number of cells was normalized to Day1 of corresponding cell line (n=3) (*p<0.05)

Furthermore, proliferation capacity was analysed via BrdU assay which determines the cells that are in S-phase during 4 hours of BrdU incubation. Analysis of BrdU positive cell population in MCF10A APTX overexpressing cells showed slightly less proliferation but the reduction compared to control cells was not significant. (Figure 3.5) The difference observed via MTT and trypan could occur because of a cumulative effect over 7 days, while momentary difference in the cells in S-phase could be subtle to be detected by BrdU incorporation assay.

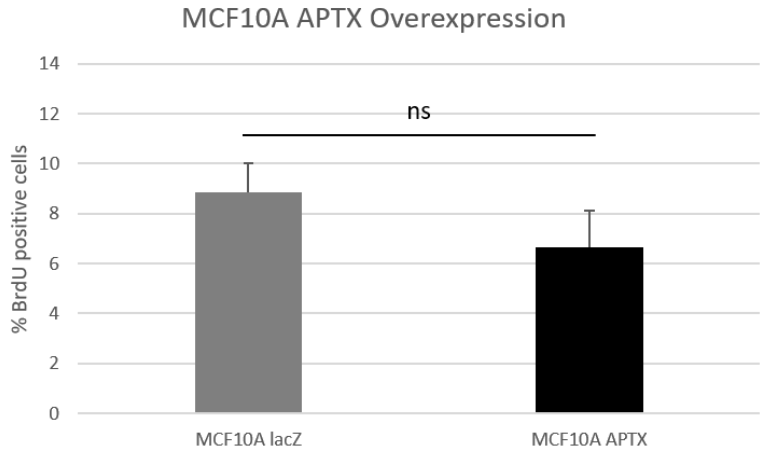

Figure 3.5 BrdU positive cell percentages were calculated in MCF10A cells after 4 hours of BrdU incorporation. (n=3)

3.3 APTX overexpresion triggers G2/M arrest in MCF10A cells

For investigation of cell cycle profile, collected MCF10A APTX overexpressing cells were stained by Propidium Iodide. Cell population in G2 phase significantly increased with APTX upregulation as 18.6% than LacZ cells with 15.3%. Reduced percentage in G1 phase correlates with G2/M phase arrest. Also, moderately enhanced S phase is parallel to findings in the experiments testing proliferation rates. (Figure 3.6) Similar to BrdU assay, difference can be revealed in stress-induced environment.

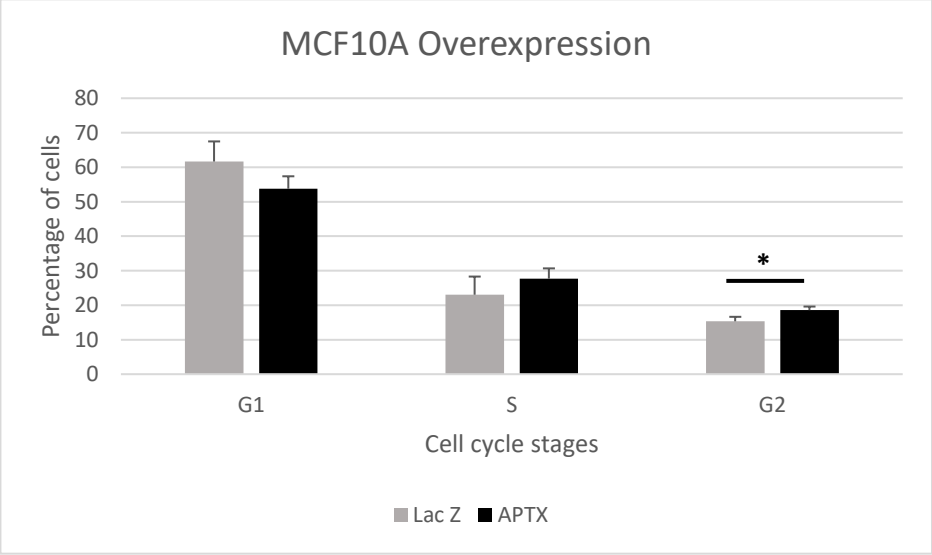

Figure 3.6 Effect of APTX overexpression on cell cycle distribution of MCF10A cells. Percentages of cell populations are presented as means. (n=3) (*p<0.05)

3.4 APTX overexpression facilitates Doxorubicin-induced apoptosis in MCF10A cells

Apoptotic cells were quantified by Annexin-V assay. Induction of cell death by apoptotic reagent Doxorubicin was accomplished in both MCF10A LacZ and APTX overexpressing cell lines. Increase in apoptotic cell percentage from 12.3% to 22.3%

was detected in LacZ cells while apoptosis rate raised from 7.33% to 55.7% in APTX overexpressing cells after treatment. In solvent DMSO condition, APTX overexpression resulted in significantly lower levels of apoptosis compared to LacZ cells so basal apoptosis is diminished. Further, significantly higher apoptosis rate determined in APTX upregulation with Doxorubicin shows that stress-induced apoptosis is promoted. (Figure 3.7)

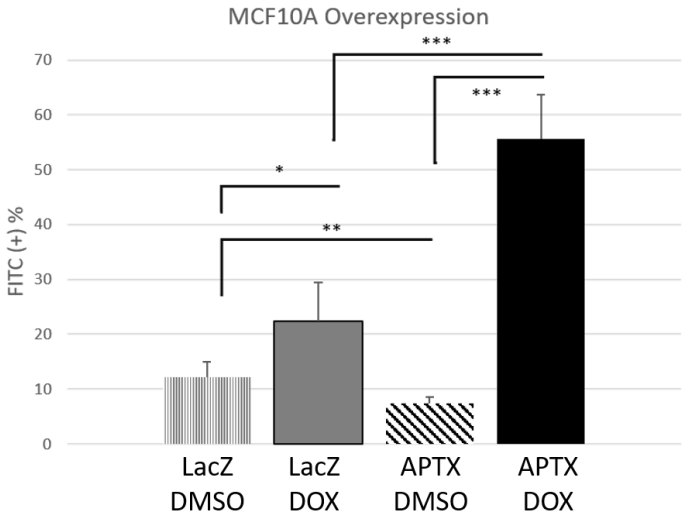

Figure 3.7 Flow cytometric quantification of apoptosis in MCF10A cells. Percentage of FITC positive cells against different treatments was indicated. (n=2) (*p<0.05, **p<0.01, ***p<0.005)

3.5 Expression analysis of p53 targets in mRNA level

Expression analysist of p53 target genes associated with proliferation, cell cycle and apoptosis was carried out by RT-qPCR. 1.95 times higher PUMA mRNA expression was demonstrated in MCF10A APTX overexpressing cells. Besides, a negligible increase in p53 and KILLER was observed. Notably, lower levels of GADD45 expression was found in case of APTX activation. (Figure 3.8)

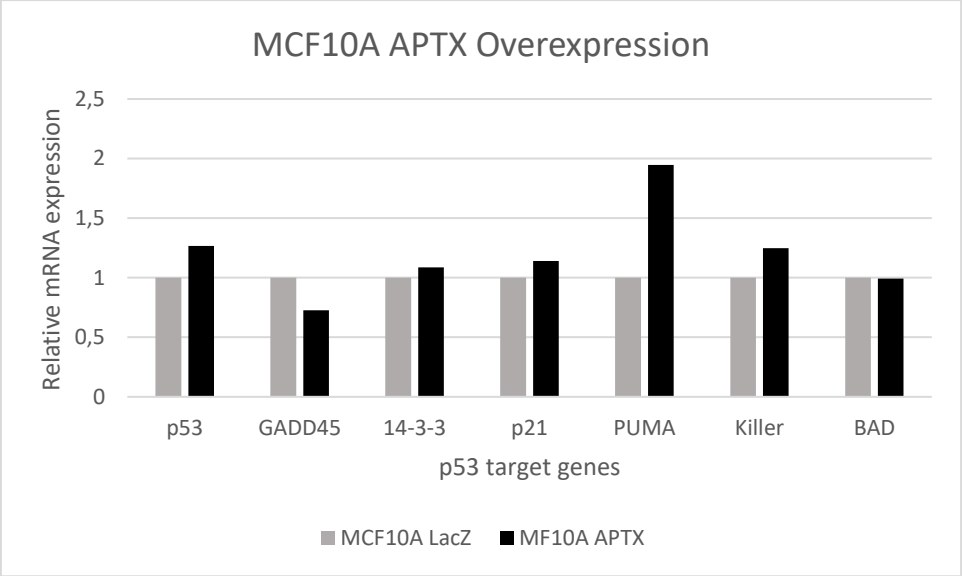

Figure 3.8 mRNA expression levels of p53 target genes were assessed in stable MCF10A cells. Fold-change was implied as compared to LacZ cells. TBP was used as the housekeeping gene for normalization. (n=1)

3.6 CRISPR-mediated APTX knockdown in MCF10A cells

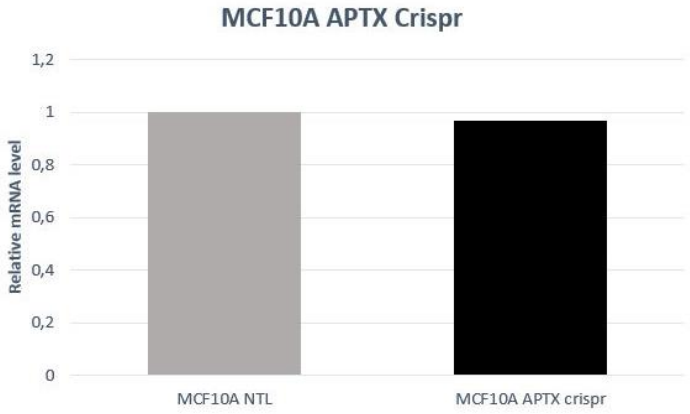

Figure 3.9 Expression analysis of stable MCF10A cells with Crispr mediated Aprataxin disruption via RT-qPCR. TBP expression was used for normalization. (n=1)

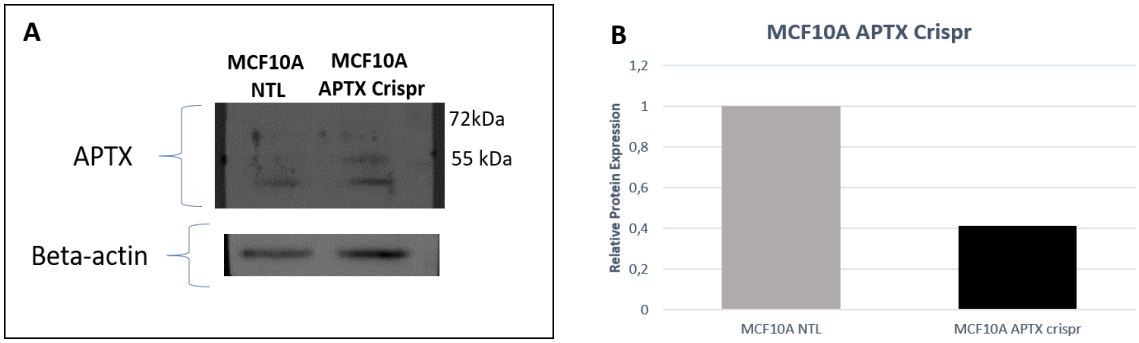

Figure 3.10 APTX knockdown in MCF10A cells. A. Downregulation of Aprataxin was verified by using APTX antibody in Western blot B. Density quantification of Aprataxin bands showed the decreased expression in stable MCF10A APTX Crispr cells compared to NTL control cells. (n=1)

APTX mRNA expression did not decrease as a consequence of Exon4-specific targeting via Crispr/Cas9 technology in MCF10A cell line (Figure 3.9). 40 kDa endogenous Aprataxin was depleted as shown in Western blot images of MCF10A-APTX Crispr cells showing 0.41 times less Aprataxin production. (Figure 3.10A and B)

3.7 Basal apoptosis rate is increased with APTX knockdown in MCF10A cells

To define apoptotic capacity of MCF10A APTX Crispr cells, Annexin V assay was performed. Here, methanol used as the solvent control because doxorubicin utilized in this experiment was dissolved in methanol. As indicated in Figure 3.11, Doxorubicin induced apoptosis in MCF10A NTL cells with 59.25% apoptotis rate compared to methanol control with 15.85%. APTX disruption caused stimulation of apoptosis even in methanol control samples with 56.6% apoptotic cells. Surprisingly, Doxorubicin treatment did not overactivate cell death mechanisms.

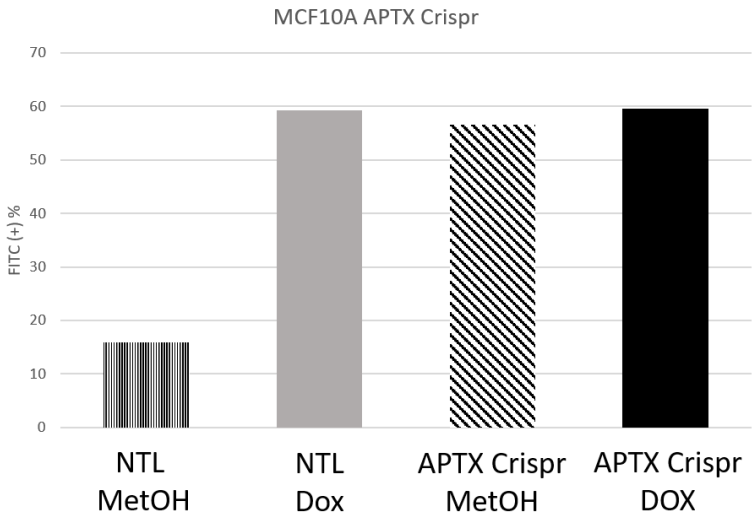

Figure 3.11 Quantification of apoptosis by Annexin V staining in MCF10A cells treated with solvent Methanol (MetOH) or Doxorubicin (n=1)

3.8 Expression analysis of p53 targets in MCF10A APTX Crispr cells

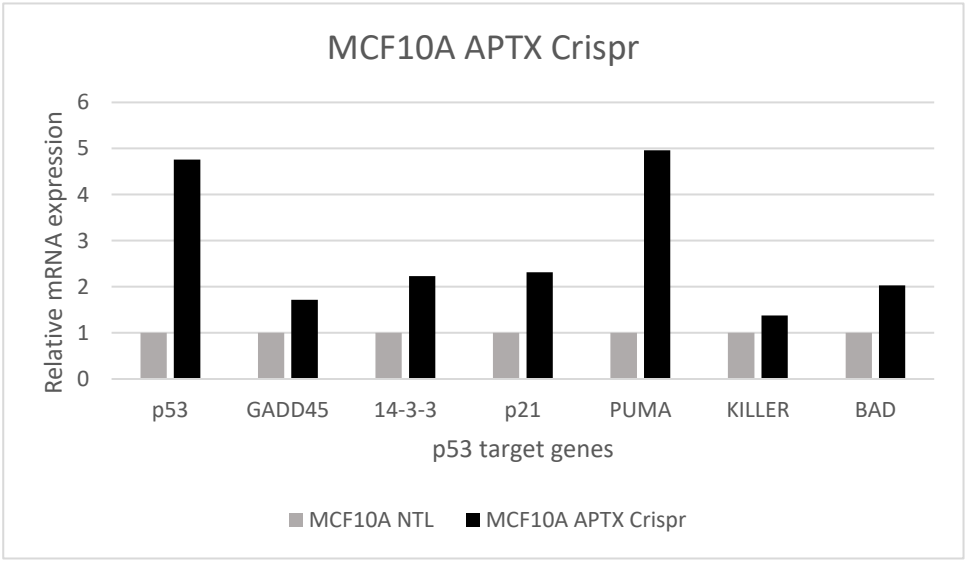

Figure 3.12 mRNA expression levels of p53 target genes were assessed in stable MCF10A Crispr cells. Fold-change was implied as compared to NTL cells. TBP was used as the housekeeping gene for normalization. (n=1)

Alteration in p53 target genes' expression was determined in APTX disrupted MCF10A cells by RT-qPCR. Induction of PUMA and p53 expression was observed in transcriptional level in 4.96 fold and 4.76 fold respectively. mRNA levels of GADD45, 14-3-3, p21, KILLER and BAD were increased on a small scale. (Figure 3.12)

3.9 CRISPR-mediated APTX knockdown was validated in MCF7 cells

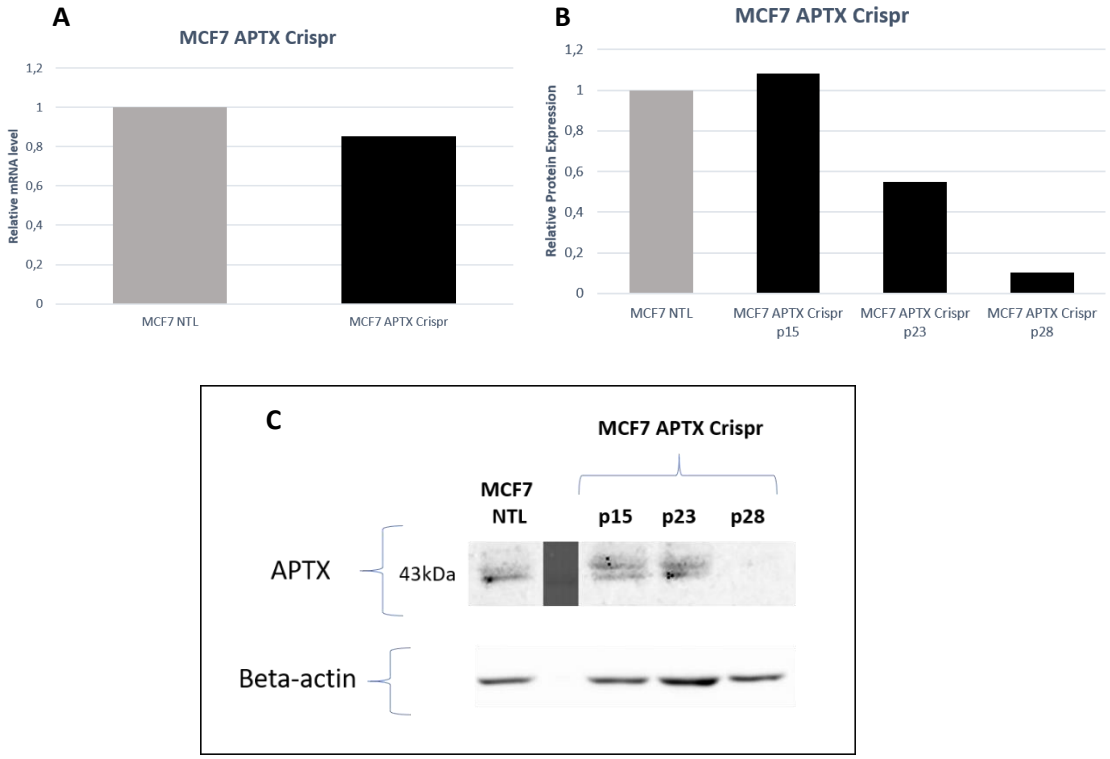

Figure 3.13 APTX knockdown in MCF7 cells was revealed in both mRNA and protein level. A. Relative APTX mRNA level suggests decrease in MCF7 APTX Crispr cells (n=1) B. Quantification of band intensities indicates a time-dependent reduction in Aprataxin. (n=1) C. Western blot image pointed out Aprataxin depletion.

To specify the effect of APTX disruption in p53 wild-type cancer cells, MCF7-APTX knockdown cells were generated by Crispr/Cas9 gene editing. Although APTX mRNA level decreased slightly in MCF7-APTX Crispr cells (Figure 3.13A), they demonstrated an obvious passage-associated reduction in protein level. This finding is consistent with constitutive expression of gRNA and Cas9. (Figure 3.13B and C)

3.10 APTX loss enhances growth in MCF7 cells

To elucidate outcomes of APTX knockdown in MCF7 cells, proliferation was checked via MTT assay. Figure 3.13 provides experimental data on relative growth of MCF7 APTX Crispr cells compared to MCF7 NTL control cells. APTX loss promoted growth of MCF7 cells signicantly on day 3 and 7. (Figure 3.14)

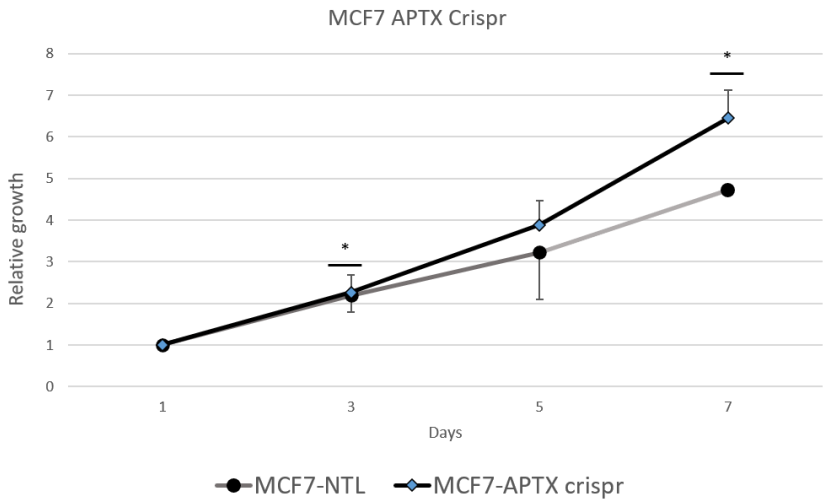

Figure 3.14 Cell viability was measured at day 1, 3, 5 and 7 performing MTT assay in MCF7 APTX Crispr cells. Absorbance of each day was normalized to Day 1 of corresponding cell line. (n=2) (*$p<0.05$)

3.11 Effect of APTX depletion on cell cycle distribution in MCF7 cells

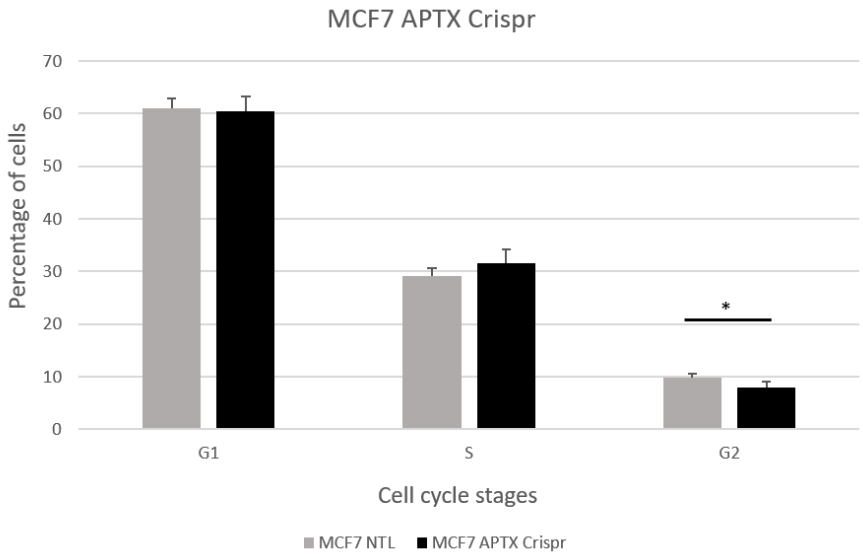

Figure 3.15 Cell cycle profile of MCF7 APTX Crispr cells. Percentages of cell populations are presented as means. (n=3) (*$p<0.05$)

Investigation of cell cycle progression suggests that percentage of cells in S-phase is greater in MCF7 APTX Crispr cells but difference is not statistically significant. There is a significant decline in the fraction of cells in G2-phase from 9.83% to 7.96%. (Figure 3.15)

3.12 Basal apoptosis rate is increased with APTX knockdown in MCF7 cells

Percentage of apoptotic cells was measured in MCF7 APTX Crispr cells. Contrary to expectations, cisplatin treatment could induce apoptosis neither in control nor in Crispr cells. Comparison of NaCl treated cells indicated that there is a slight rise in basal apoptosis rate of MCF7 APTX Crispr cells compated to NTL control. (Figure 3.16)

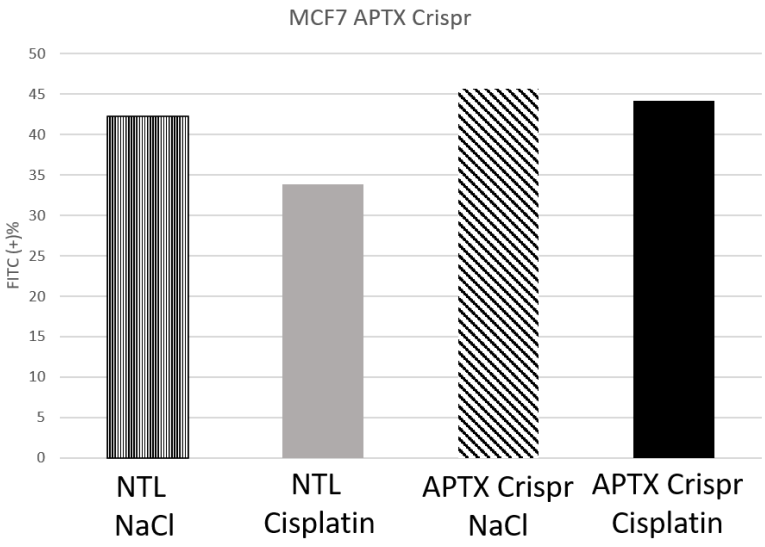

Figure 3.16 Quantification of apoptotic cells treated with solvent NaCl or Cisplatin by Annexin V staining in MCF7 cells (n=1)

3.13 Expression analysis of p53 targets in MCF7 APTX Crispr cells

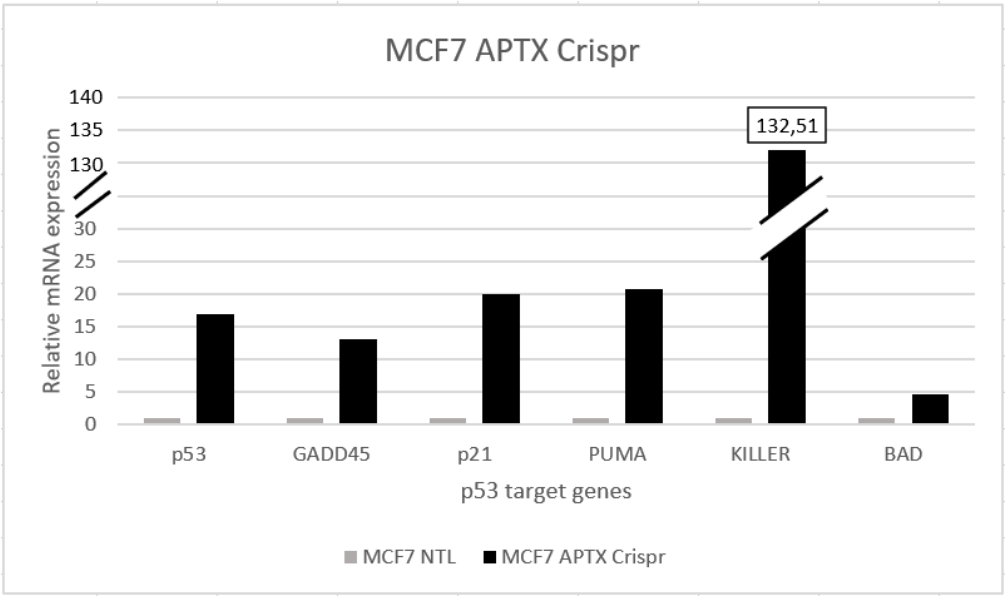

Figure 3.17 mRNA expression levels of p53 target genes were assessed in stable MCF7 Crispr cells. Fold-change was implied as compared to NTL cells. TBP was used as the housekeeping gene for normalization. (n=1)

APTX disruption leads to higher p53, GADD45, p21, PUMA transcript levels in MCF7 cells. Additionally, abundant expression of KILLER mRNA with 132.51 fold increase in MCF7 APTX Crispr cells compared MCF7 NTL cells. On the other hand, moderately elevated BAD mRNA expression was identified. (Figure 3.17)

CHAPTER 4

DISCUSSION AND CONCLUSION

Aprataxin is a nucleotide deadenylase which eliminates abortive ligation substrates. It is recruited to damaged sites interacting with XRCC repair proteins.[31] Considering its association with repair complexes, discovery of its molecular interaction with p53 was not surprising. Although role of Aprataxin in DNA repair and neurodegenerative diseases is established well, its impact on other p53-related pathways has not been investigated in detail. p53 is present in mutant form in many cancer but cancer cells expressing wild-type p53 with defective p53 activation also gives rise to pro-oncogenic activities.[3] Several findings confirmed that redox-sensitive proteins affect p53 stabilization.[15, 16] Aprataxin is one of the candidates suggested by a study covering changes in p53 activity as a response to antioxidant protein mutations.[17] Here with this study, we aimed to reveal the importance of Aprataxin in p53-mediated fundamental pathways including proliferation, cell cycle and apoptosis.

Firstly, Aprataxin overexpression was induced in p53-WT normal human breast cells MCF10A. Significantly increased viability was found in MCF10A-APTX cells at day 7 of the MTT and Trypan counting experiments. However, BrdU assay demonstrated no difference in proliferating cell rate between APTX overexpressing cells and LacZ control cells. This assay is performed on fixed cells that were exposed to BrdU for 4 hours to detect cells in S-phase. APTX overexpression might render those cells less sensitive to cumulative damage so this experiment can be carried out under stress conditions such as nutrient deprivation or accumulated external/internal stress stimuli with long-term culture. It would support the protective role of Aprataxin because damaging factors are accumulated in the environment over time. Cell cycle analysis indicated G2/M phase arrest in MCF10A-APTX cells while basal apoptosis rate is significantly reduced compared to control in parallel. On the contrary, Doxorubicin-induced apoptosis was stimulated significantly higher in MCF10A-APTX cells.

According to these data, we can infer that Aprataxin provokes growth arrest preventing cell death in low stress levels but apoptosis is significantly activated in stressed conditions with oxidative damage. A possible explanation for the difference can be due to accumulation of p53 levels in response to Doxorubicin treatment which increases the possibility of Aprataxin interaction with p53. Moderate increase in pro-apoptotic PUMA mRNA level can be provoked with Doxorubicin treatment.

Besides, several isoforms of Aprataxin with different sizes have been discovered so far.[20] The form which was expressed in MCF10A cells after transduction is 30kDa. This isoform might be lack of critical parts of FHA or HIT domain which intreact with p53. Interaction between p53 and Aprataxin should be investigated in the context of domain-specific functions.

Next, apoptotic signaling mechanisms were examined in MCF10A-APTX Crispr cells to find out the effect of APTX knockdown on apoptotic response. Based on analysis of cells treated with DMSO, APTX disruption generates higher apoptotic cell number at the basal level compared to NTL control cells. This finding is consistent with literature because continuous passage of Aptx -/- mouse embryonic fibroblasts over 10 passages leads to delay in growth and accelerated senescence due to accumulation of DNA lesions. Similarly, limited transcription recovery was detected with radiolabelled nucleotides after oxidative stress exposure.[34] Increase in PUMA and p53 mRNA levels seems to be consistent with Annexin V assay results. Alternatively, it may represent p53-independent induction of apoptosis. Quantification of p53 and associated pro-apoptotic proteins would be more enlightening. Functional studies concerning apoptosis with p53 suppression in APTX Crispr cells is further required to uncover whether p53 is essential to sustain cell death in this mechanism.

Since absence of enzymatic function of Aprataxin can be restored by compensatory mechanisms, outcome of APTX disruption can be originated from direct interaction with p53 or indirect control of p53 interacting partners.[28] If p53 and Aprataxin creates a complex which has an impact on p53 protein stabilization and conformation, alterations in p53 downstream targets is expected in APTX Crispr cells. Deleterious effect of APTX knockdown could be attributed to robust production of intracellular ROS emerged from downregulation of APE1/NRF1/NRF2 pathway.[35, 41] NRF2 facilitates transcription of MDM2 which is the negative regulator of p53.[15]

Therefore, inactivation of MDM2 through NRF2 reduction may lead to p53 stabilization in this case. Likewise, some studies showed that siNRF2 treated cells enhanced p53 expression.[42] To approve this assumption, p53 and PUMA stimulation can be tested in protein level along with APE1/NRFs pathway interacting proteins. The most likely cause of extensive apoptosis can be explained in this way. Although repression of p53 activity mediated by MDM2 has been found in protein level, site-specific phosphorylation of MDM2 improves binding to p53 mRNA promoting p53 production acting as a positive regulator.[43] Additional post-translational modifications of MDM2 that regulate p53 expression might exist considering higher p53 and PUMA trancripts. Moreover, both control and MCF10A APTX Crispr cells undergo apoptosis in a similar level after incubation with Doxorubicin. Despite drug exposure promoted apoptosis in MCF10A NTL cells, there was no change in proportion of apoptotic cells with Doxorubicin treated MCF10A-APTX Crispr cells compared to DMSO treatment. Similar levels of FITC positive cells might be arised from hyperactivated basal cell death.

MCF7 APTX Crispr cells were monitored by MTT assay and significantly increased viability was revealed compared to NTL cells. Significant reduction in G2 phase may represent S-phase arrest. Prior studies have noted that HNT3 loss brings about growth arrest due to activation of S-phase checkpoint in budding yeast with induced mis-incorporated ribonucleotides, as well.[27] However, increase in S-phase is not sufficient to draw a clear conclusion. In order to achieve a more accurate cell cycle analysis, synchronization can be applied. This method inhibits cell cycle progression to obtain cell populations at a specific cell cycle phase.[44] Since dysregulation of cell cycle is common feature of cancer cells, identification of growth arrest is crucial. [45]

Furthermore, basal cell death is elevated in MCF7 APTX Crispr cells. Regarding transcript levels of p53 targets, APTX loss especially enhanced KILLER mRNA level as 132.5 fold in MCF7 cells. KILLER, also called Death Receptor-5 controlled by p53, activates procaspases for initiation of death-executing cascade.[46] Thereby, the sharp increase in KILLER level might refer to extrinsic apoptosis triggered by APTX disruption. Other downstream genes displayed 15-20 fold higher expression in MCF7 APTX Crispr cells compared to NTL cells except BAD with 5 fold increase. All p53 targets examined in this study must be analyzed at protein level to clarify whether

change of their expression is under control of p53. Also, expression analysis and other assays should be performed with stress induction such as H_20_2 or genotoxic agent treatment. For instance, APTX deletion creates impaired survival and repair in SOD1 mutant mouse model which overproduce DNA damage owing to oxidative environment.[34] Hence, p53/Aprataxin interplay responding against damage can elucidate the importance of APTX in p53-dependent pathways.

Previously published studies implicated that radio/chemoresistance can be coordinated by Aprataxin.[38, 39, 47] Reports demonstrate lower levels of NRF2 and OPA1 as a consequence of APTX disruption strongly support this hypothesis. Because the deletion of OPA1 leads to reduced resistance and promotes angiogenesis while targeting NRF2 may sensitize cancer cells.[48-50] To evaluate this possibility in breast cancer, apoptosis should be assesed in MCF7 APTX Crispr cells with higher concentration of cisplatin or other apoptosis inducing agents. Also, complete APTX knockout can be tested in these cells. Additionally, breast cancer patient screening that focus on drug sensitivity and survival rate might be carried out.

Immunostaining of Aprataxin showed nuclear localization in breast cells. (data not shown) However, impact of APTX on regulation of downstream signaling pathways may control mitochondrial morphology and function. Taking into account the defective mitochondrial properties in APTX deficient cells, changes of this dynamic organelle during carcinogenesis can be investigated in comparative studies using APTX disrupted breast cells.[29, 35] Results might allow us to evaluate the role of p53-Aprataxin interaction on oxidative stress response, apoptosis and metabolism reprogramming.

In a nutshell, Aprataxin protects cells against internal damage by triggering cell cycle arrest but it also stimulates apoptosis to eliminate detrimental outcomes of severe stress. APTX disruption gives rise to cell death even without stress factors. Especially, KILLER overexpression observed in MCF7 cells is intriguing. This finding, while preliminary, suggests that extrinsic apoptosis pathway might be activated. To rule out p53-independent regulation of those processes, further research should be carried out under stress conditions and taking p53 protein levels into account.

REFERENCES

1. Sun, Z., The General Information of the Tumor Suppressor Gene p53 and the Protein p53. *Journal of Cancer Prevention & Current Research* 2015, *3*.

2. Linzer, D. I.; Levine, A. J., Characterization of a 54K dalton cellular SV40 tumor antigen present in SV40-transformed cells and uninfected embryonal carcinoma cells. *Cell* 1979, *17* (1), 43-52.

3. Donehower, L. A.; Harvey, M.; Slagle, B. L.; McArthur, M. J.; Montgomery, C. A.; Butel, J. S.; Bradley, A., Mice deficient for p53 are developmentally normal but susceptible to spontaneous tumours. *Nature* 1992, *356* (6366), 215-221.

4. Levine, A. J.; Hu, W.; Feng, Z., The P53 pathway: what questions remain to be explored? *Cell Death & Differentiation* 2006, *13* (6), 1027-1036.

5. Taylor, W. R.; Stark, G. R., Regulation of the G2/M transition by p53. *Oncogene* 2001, *20* (15), 1803-15.

6. Benzinger, A.; Muster, N.; Koch, H. B.; Yates, J. R., 3rd; Hermeking, H., Targeted proteomic analysis of 14-3-3 sigma, a p53 effector commonly silenced in cancer. *Mol Cell Proteomics* 2005, *4* (6), 785-95.

7. Zhang, J.; Huang, K.; O'Neill, K. L.; Pang, X.; Luo, X., Bax/Bak activation in the absence of Bid, Bim, Puma, and p53. *Cell Death Dis* 2016, *7* (6), e2266.

8. Brown, C. J.; Lain, S.; Verma, C. S.; Fersht, A. R.; Lane, D. P., Awakening guardian angels: drugging the p53 pathway. *Nat Rev Cancer* 2009, *9* (12), 862-73.

9. Offer, H.; Zurer, I.; Banfalvi, G.; Reha'k, M.; Falcovitz, A.; Milyavsky, M.; Goldfinger, N.; Rotter, V., p53 modulates base excision repair activity in a cell cycle-specific manner after genotoxic stress. *Cancer Res* 2001, *61* (1), 88-96.

10. Williams, A. B.; Schumacher, B., p53 in the DNA-Damage-Repair Process. *Cold Spring Harb Perspect Med* 2016, *6* (5), a026070.

11. Fridman, J. S.; Lowe, S. W., Control of apoptosis by p53. *Oncogene* 2003, *22* (56), 9030-9040.

12. Lakin, N. D.; Jackson, S. P., Regulation of p53 in response to DNA damage. *Oncogene* 1999, *18* (53), 7644-7655.

13. Oren, M., Regulation of the p53 tumor suppressor protein. *J Biol Chem* 1999, *274* (51), 36031-4.

14. Amaral, J. D.; Xavier, J. M.; Steer, C. J.; Rodrigues, C. M., The role of p53 in apoptosis. *Discov Med* 2010, *9* (45), 145-52.

15. Eriksson, S. E.; Ceder, S.; Bykov, V. J. N.; Wiman, K. G., p53 as a hub in cellular redox regulation and therapeutic target in cancer. *J Mol Cell Biol* 2019, *11* (4), 330-341.

16. Sengupta, S.; Mitra, S.; Bhakat, K. K., Dual regulatory roles of human AP-endonuclease (APE1/Ref-1) in CDKN1A/p21 expression. *PLoS One* 2013, *8* (7), e68467-e68467.

17. Bekki, G. Regulation of Human p53 tumor suppressor gene activity by thiol-dependent oxidoreductases. Izmir Institute of Technology, 2011.

18. Sykora, P.; Croteau, D. L.; Bohr, V. A.; Wilson, D. M., Aprataxin localizes to mitochondria and preserves mitochondrial function. *Proceedings of the National Academy of Sciences* 2011, *108* (18), 7437.

19. Jiang, B.; Glover, J. N. M.; Weinfeld, M., Neurological disorders associated with DNA strand-break processing enzymes. *Mech Ageing Dev* 2017, *161* (Pt A), 130-140.

20. Sano, Y.; Date, H.; Igarashi, S.; Onodera, O.; Oyake, M.; Takahashi, T.; Hayashi, S.; Morimatsu, M.; Takahashi, H.; Makifuchi, T.; Fukuhara, N.; Tsuji, S., Aprataxin, the causative protein for EAOH is a nuclear protein with a potential role as a DNA repair protein. *Annals of Neurology* 2004, *55* (2), 241-249.

21. Becherel, O. J.; Jakob, B.; Cherry, A. L.; Gueven, N.; Fusser, M.; Kijas, A. W.; Peng, C.; Katyal, S.; McKinnon, P. J.; Chen, J.; Epe, B.; Smerdon, S. J.; Taucher-Scholz, G.; Lavin, M. F., CK2 phosphorylation-dependent interaction between aprataxin and MDC1 in the DNA damage response. *Nucleic Acids Res* 2010, *38* (5), 1489-1503.

22. Gueven, N.; Becherel, O. J.; Kijas, A. W.; Chen, P.; Howe, O.; Rudolph, J. H.; Gatti, R.; Date, H.; Onodera, O.; Taucher-Scholz, G.; Lavin, M. F., Aprataxin, a novel protein that protects against genotoxic stress. *Hum Mol Genet* 2004, *13* (10), 1081-93.

23. Harris, J. L.; Jakob, B.; Taucher-Scholz, G.; Dianov, G. L.; Becherel, O. J.; Lavin, M. F., Aprataxin, poly-ADP ribose polymerase 1 (PARP-1) and apurinic endonuclease 1 (APE1) function together to protect the genome against oxidative damage. *Hum Mol Genet* 2009, *18* (21), 4102-17.

24. Rass, U.; Ahel, I.; West, S. C., Actions of aprataxin in multiple DNA repair pathways. *J Biol Chem* 2007, *282* (13), 9469-74.

25. Becherel, O. J.; Gueven, N.; Birrell, G. W.; Schreiber, V.; Suraweera, A.; Jakob, B.; Taucher-Scholz, G.; Lavin, M. F., Nucleolar localization of aprataxin is dependent on interaction with nucleolin and on active ribosomal DNA transcription. *Human Molecular Genetics* 2006, *15* (14), 2239-2249.

26. Schellenberg, M. J.; Tumbale, P. P.; Williams, R. S., Molecular underpinnings of Aprataxin RNA/DNA deadenylase function and dysfunction in neurological disease. *Prog Biophys Mol Biol* 2015, *117* (2-3), 157-165.

27. Tumbale, P.; Williams, J. S.; Schellenberg, M. J.; Kunkel, T. A.; Williams, R. S., Aprataxin resolves adenylated RNA-DNA junctions to maintain genome integrity. *Nature* 2014, *506* (7486), 111-5.

28. Çaglayan, M.; Prasad, R.; Krasich, R.; Longley, M. J.; Kadoda, K.; Tsuda, M.; Sasanuma, H.; Takeda, S.; Tano, K.; Copeland, W. C.; Wilson, S. H., Complementation of aprataxin deficiency by base excision repair enzymes in mitochondrial extracts. *Nucleic Acids Res* 2017, *45* (17), 10079-10088.

29. Zheng, J.; Croteau, D. L.; Bohr, V. A.; Akbari, M., Diminished OPA1 expression and impaired mitochondrial morphology and homeostasis in Aprataxin-deficient cells. *Nucleic Acids Res* 2019, *47* (8), 4086-4110.

30. Ababneh, N. A.; Ali, D.; Al-Kurdi, B.; Sallam, M.; Alzibdeh, A. M.; Salah, B.; Ryalat, A. T.; Azab, B.; Sharrack, B.; Awidi, A., Identification of APTX disease-causing mutation in two unrelated Jordanian families with cerebellar ataxia and sensitivity to DNA damaging agents. *PLoS One* 2020, *15* (8), e0236808.

31. Luo, H.; Chan, D. W.; Yang, T.; Rodriguez, M.; Chen, B. P.; Leng, M.; Mu, J. J.; Chen, D.; Songyang, Z.; Wang, Y.; Qin, J., A new XRCC1-containing complex and its role in cellular survival of methyl methanesulfonate treatment. *Mol Cell Biol* 2004, *24* (19), 8356-65.

32. El-Khamisy, S. F.; Katyal, S.; Patel, P.; Ju, L.; McKinnon, P. J.; Caldecott, K. W., Synergistic decrease of DNA single-strand break repair rates in mouse neural cells lacking both Tdp1 and aprataxin. *DNA Repair (Amst)* 2009, *8* (6), 760-6.

33. Reynolds, J. J.; El-Khamisy, S. F.; Katyal, S.; Clements, P.; McKinnon, P. J.; Caldecott, K. W., Defective DNA ligation during short-patch single-strand break repair in ataxia oculomotor apraxia 1. *Molecular and cellular biology* 2009, *29* (5), 1354-1362.

34. Carroll, J.; Page, T. K.; Chiang, S. C.; Kalmar, B.; Bode, D.; Greensmith, L.; McKinnon, P. J.; Thorpe, J. R.; Hafezparast, M.; El-Khamisy, S. F., Expression of a pathogenic mutation of SOD1 sensitizes aprataxin-deficient cells and mice to oxidative stress and triggers hallmarks of premature ageing. *Hum Mol Genet* 2015, *24* (3), 828-40.

35. Garcia-Diaz, B.; Barca, E.; Balreira, A.; Lopez, L. C.; Tadesse, S.; Krishna, S.; Naini, A.; Mariotti, C.; Castellotti, B.; Quinzii, C. M., Lack of aprataxin impairs mitochondrial functions via downregulation of the APE1/NRF1/NRF2 pathway. *Hum Mol Genet* 2015, *24* (16), 4516-29.

36. Friedler, A.; Veprintsev, D. B.; Rutherford, T.; von Glos, K. I.; Fersht, A. R., Binding of Rad51 and other peptide sequences to a promiscuous, highly electrostatic binding site in p53. *J Biol Chem* 2005, *280* (9), 8051-9.

37. Sánchez-Puig, N.; Veprintsev, D. B.; Fersht, A. R., Binding of natively unfolded HIF-1alpha ODD domain to p53. *Mol Cell* 2005, *17* (1), 11-21.

38. Dopeso, H.; Mateo-Lozano, S.; Elez, E.; Landolfi, S.; Ramos Pascual, F. J.; Hernández-Losa, J.; Mazzolini, R.; Rodrigues, P.; Bazzocco, S.; Carreras, M. J.; Espín, E.; Armengol, M.; Wilson, A. J.; Mariadason, J. M.; Ramon, Y. C. S.; Tabernero, J.; Schwartz, S., Jr.; Arango, D., Aprataxin tumor levels predict response of colorectal cancer patients to irinotecan-based treatment. *Clin Cancer Res* 2010, *16* (8), 2375-82.

39. Wang, X.; Li, Q.; Jin, H.; Zou, H.; Xia, W.; Dai, N.; Dai, X.-Y.; Wang, D.; Xu, C.-X.; Qing, Y., miR-424 acts as a tumor radiosensitizer by targeting aprataxin in cervical cancer. *Oncotarget* 2016, *7* (47), 77508-77515.

40. Shalem, O.; Sanjana, N. E.; Hartenian, E.; Shi, X.; Scott, D. A.; Mikkelson, T.; Heckl, D.; Ebert, B. L.; Root, D. E.; Doench, J. G.; Zhang, F., Genome-scale CRISPR-Cas9 knockout screening in human cells. *Science* 2014, *343* (6166), 84-87.

41. Leung, L.; Kwong, M.; Hou, S.; Lee, C.; Chan, J. Y., Deficiency of the Nrf1 and Nrf2 transcription factors results in early embryonic lethality and severe oxidative stress. *J Biol Chem* 2003, *278* (48), 48021-9.

42. Ko, H.; Kim, S. J.; Shim, S. H.; Chang, H.; Ha, C. H., Shikonin Induces Apoptotic Cell Death via Regulation of p53 and Nrf2 in AGS Human Stomach Carcinoma Cells. *Biomol Ther (Seoul)* 2016, *24* (5), 501-9.

43. Karakostis, K.; Fåhraeus, R., Shaping the regulation of the p53 mRNA tumour suppressor: the co-evolution of genetic signatures. *BMC Cancer* 2019, *19* (1), 915.

44. Sonoda, E., Synchronization of cells. *Subcell Biochem* 2006, *40*, 415-8.

45. Hartwell, L. H.; Kastan, M. B., Cell cycle control and cancer. *Science* 1994, *266* (5192), 1821-8.

46. Wu, G. S.; Burns, T. F.; McDonald, E. R., 3rd; Jiang, W.; Meng, R.; Krantz, I. D.; Kao, G.; Gan, D. D.; Zhou, J. Y.; Muschel, R.; Hamilton, S. R.; Spinner, N. B.; Markowitz, S.; Wu, G.; el-Deiry, W. S., KILLER/DR5 is a DNA damage-inducible p53-regulated death receptor gene. *Nat Genet* 1997, *17* (2), 141-3.

47. Shen, J.; Wei, J.; Wang, H.; Yue, G.; Yu, L.; Yang, Y.; Xie, L.; Zou, Z.; Qian, X.; Ding, Y.; Guan, W.; Liu, B., A three-gene signature as potential predictive biomarker for irinotecan sensitivity in gastric cancer. *J Transl Med* 2013, *11*, 73.

48. Herkenne, S.; Scorrano, L., OPA1, a new mitochondrial target in cancer therapy. *Aging (Albany NY)* 2020, *12* (21), 20931-20933.

49. Li, D.; Hong, X.; Zhao, F.; Ci, X.; Zhang, S., Targeting Nrf2 may reverse the drug resistance in ovarian cancer. *Cancer Cell Int* 2021, *21* (1), 116.

50. Roh, J. L.; Kim, E. H.; Jang, H.; Shin, D., Nrf2 inhibition reverses the resistance of cisplatin-resistant head and neck cancer cells to artesunate-induced ferroptosis. *Redox Biol* 2017, *11*, 254-262.